Redesigning Channel-Forming Peptides: Amino Acid Substitutions that Enhance Rates of Supramolecular Self-Assembly and Raise Ion Transport Activity

Lalida P. Shank,* James R. Broughman,*† Wade Takeguchi,* Gabriel Cook,* Ashley S. Robbins,* Lindsey Hahn,* Gary Radke,* Takeo Iwamoto,* Bruce D. Schultz,† and John M. Tomich*
*Department of Biochemistry, and †Department of Anatomy and Physiology, Kansas State University, Manhattan, Kansas 66506

ABSTRACT Three series of 22-residue peptides derived from the transmembrane M2 segment of the glycine receptor α1-subunit (M2GlyR) have been designed, synthesized, and tested to determine the plasticity of a channel-forming sequence and to define whether channel pores with enhanced conductive properties could be created. Sixteen sequences were examined for aqueous solubility, solution-association tendency, secondary structure, and half-maximal concentration for supramolecular assembly, channel activity, and ion transport properties across epithelial monolayers. All peptides interact strongly with membranes: associating with, inserting across, and assembling to form homooligomeric bundles when in micromolar concentrations. Single and double amino acid replacements involving arginine and/or aromatic amino acids within the final five C-terminal residues of the peptide cause dramatic effects on the concentration dependence, yielding a range of $K_{1/2}$ values from 36 $\pm$ 5 to 390 $\pm$ 220 μM for transport activity. New water/lipid interfacial boundaries were established for the transmembrane segment using charged or aromatic amino acids, thus limiting the peptides' ability to move perpendicularly to the plane of the bilayer. Formation of discrete water/lipid interfacial boundaries appears to be necessary for efficient supramolecular assembly and high anion transport activity. A peptide sequence is identified that may show efficacy in channel replacement therapy for channelopathies such as cystic fibrosis.

INTRODUCTION

A variety of ionophores and channels are available to dissipate electrical and/or chemical gradients across cell membranes for therapeutic, industrial, and research purposes. For example, valinomycin is widely employed as a K^+ selective ionophore to dissipate chemical gradients across cell membranes, monensin has been used to selectively dissipate Na^+ gradients, and A23187 has been used in protocols to increase cytosolic Ca^{2+}. Unfortunately, there are no commercially available anion-selective ionophores or channels that can be topically applied from purely aqueous solutions. The development of chloride selective pores would find applied use in the clinic for treating channelopathies such as cystic fibrosis, and in basic research by producing anionophores that modulate counterion movement when studying cation channels. In a recent review on artificial channels for Na^+ and K^+, it was observed (1) that peptide-based channel designs achieved high unitary conductance but low selectivity whereas chemically synthesized ion-specific macrocycles show high selectivity but low transport rates. Native protein channels can simultaneously exhibit relatively high conductance and anion/cation selectivity. These observations suggest that studies need to be conducted to explore whether or not these deficiencies in the synthetic channels can be overcome.

In our laboratory we have approached the issue of understanding chloride selectivity in a biological setting by focusing on sequence variants of the 23 amino acid, second transmembrane segment (TM2) of the α1-subunit of the spinal cord glycine receptor (M2GlyR, PARVGLGITTVL TMTTQSSGSRA) (2,3). Over 200 sequences have been chemically synthesized and analyzed for increased aqueous solubility, decreased solution associations, and reduced concentrations for supramolecular assembly rates. Early sequences adducted varying numbers of lysine residues on one of the peptide termini (4). The highly soluble CK_4-M2GlyR-p27 (PARVGLGITTVLTMTTQSSGSRAKKKK) and NK_4-M2GlyR- p27 (KKKKPARVGLGITTVLTMTTQ SSGSRA) peptides displayed preferred ion transport activities, as evidenced by their ability to permit anion secretion (measured as short-circuit current, *Isc* across confluent

Submitted July 5, 2005, and accepted for publication December 9, 2005.

Address reprint requests to Professor John M. Tomich, Dept. of Biochemistry, Kansas State University, Manhattan, KS 66506. Tel.: 785-532-5956; Fax: 785-532-6297; E-mail: jtomich@ksu.edu.

James R. Broughman's present address is Dept. of Integrative Biology, University of Texas Health Science Center, Houston, TX 77030.

Abbreviations used: CF, cystic fibrosis; WT, wild type; TFE, 2,2,2-trifluoroethanol; 1-EBIO, 1-ethyl-2-benzimidazolinone; M2GlyR, second transmembrane sequence of the α1 subunit of the glycine receptor from spinal cord; TM, transmembrane; MDCK, Madin-Darby canine kidney cells; *Isc*, short circuit current, NMR, nuclear magnetic resonance; MW, molecular weight; FMOC, 9-fluorenylmethoxycarbonyl; HMP, *p*-hydroxymethyl-phenoxymethyl; HPLC, high performance liquid chromatography; TFA, trifluoroacetic acid; CD, circular dichroism; MALDI-TOF, matrix assisted-laser absorption time of flight mass spectroscopy; DI, deionized; BS^3, Bis [sulfosuccinimidyl] suberate; HEPES, 4-(2-hydroxyethyl) piperazine-1-ethanesulfonic acid; NMDG Cl *N*-methyl-D-glucosamine-Cl; EDTA, ethylenediamine-tetracetic acid; SDS, sodium dodecylsulfate; PAGE, polyacrylamide gel electrophoresis; POPC, (1-palmitoyl-2-oleoyl-*sn*-glycero-3-phosphocholine); POPG, (1-palmitoyl-2-oleoyl-*sn*-glycero-3-phospho-rac-(1-glycerol)).

0006-3495/06/03/2138/13 $2.00

doi: 10.1529/biophysj.105.070078

epithelial monolayers) and pharmacological responses that were similar to those seen with the parent M2GlyR sequence (2,3). However the NK_4- sequence displayed higher transport activity even though it formed higher molecular weight aggregates relative to the CK_4- peptide (5,6). NMR studies revealed that the lysines in the CK_4- peptide formed a capping structure that led to a misfolding of the sequence with a concomitant reduction in activity (7). Since this discovery nearly all of our subsequent designs have focused on the NK_4- peptides where the lysines are mobile and do not interact with the TM segment.

A series of NK_4-M2GlyR peptides were subsequently synthesized with deletions at the nonadducted terminus. Truncated NK_4-M2GlyR peptides consisting of 22–26 amino acids (i.e., 1–5 amino acids absent from the C-terminus) yielded fully active peptide assemblies (8). In the process of truncating the NK_4-adducted native sequence, a number of hydrophilic residues were omitted as defined by the Wimley and White hydrophobicity scales developed for transmembrane sequences (9–12). The increase in hydrophobicity is reflected in the reduced solubility of the deletion peptides. Among the residues removed was Arg-22 in the C-terminus of the parent M2 sequence. It has been postulated, based on solution NMR studies in dodecyl phosphatidyl choline micelles, that the registry of the wild-type transmembrane segment is defined by residues Arg-3 and Arg-22, thereby defining an 18-residue TM segment (13,14). Examining the crystal structures of membrane proteins, arginine is often located at the water/lipid interface in TM segments (15–17). Without the C-terminal arginine in the M2GlyR-p22 sequence, both ion selectivity and positioning or registry of the TM segment within the acyl lipid core are potentially compromised. Therefore, this study was initiated to evaluate the effects on channel transport properties of reintroducing an arginine at positions near the new carboxyl-terminus. Arginine residues were introduced individually at positions 18–22 and assayed for induced anion transport across MDCK monolayers. In the second and third sets of experiments double amino acid replacements were generated with aromatic amino acids placed at or near the C-terminus along with arginines at positions 19–22.

In addition to the arginine replacements other aromatic amino acids (tyrosine, tryptophan, and phenylalanine) were placed at or adjacent to the C-terminus. Aromatic residues have been observed in numerous TM segments at the aqueous/lipid interface (18–21). In a recently published study (22), we observed that substituting Ser-22 in NK_4-M2GlyR-p22 with tryptophan, was associated with decreased self-association in solution. Multidimensional proton NMR studies revealed that the tryptophan alters the solution structure of the peptide such that a new fold containing a hydrophobic cleft is generated. Based on CD studies, upon binding to membranes the tryptophan-containing peptide spontaneously refolds, adopting a more helical secondary structure.

The tryptophan substituted NK_4-M2GlyR-p22, S22W, showed several differences with regard to the maximal short circuit current (Isc_{MAX}) and the concentration dependence for one-half maximal short circuit current ($K_{1/2}$). Comparing the full-length NK_4-M2GlyR-p27, with the truncated NK_4-M2GlyR-p22 and the substituted NK_4-M2GlyR-p22 S22W, Isc_{MAX} values of 26.2 $\pm$ 5.7, 23.7 $\pm$ 5.6, and 13.0 $\pm$ 1.0 μA cm^{-2} were measured, respectively. In contrast, the concentrations for $K_{1/2}$ were 271 $\pm$ 71, 210 $\pm$ 70, and 44 $\pm$ 5.9 μM, respectively. The substituted NK_4-M2GlyR-p22 S22W sequence was able to assemble more easily, however, there appears to be a cost with regard to the maximum permeation rate.

In this report, biochemical and electrophysiological results demonstrate that the NK_4-M2GlyR-p22 sequence can be modified to bring about a variety of new bio-based channels with improved rates of supramolecular assembly with a large ensemble of conductances. In the companion paper, three of these substituted sequences were modeled in different hydrophobic environments.

EXPERIMENTAL SECTION

Peptide synthesis

All peptides were synthesized using solid phase methods employing the 9-fluorenylmethoxycarbonyl (Fmoc) amino protection strategy, as described previously (16). All peptides were purified by reversed-phase HPLC and characterized by both matrix assisted-laser desorption time-of-flight mass spectroscopy (MALDI-TOF) and ESI ion-trap mass spectroscopy.

Solubility studies

The solubility of the different peptides was determined using a previously published method (20). Briefly, saturated solutions of the crude peptides in a modified Ringer solution ''A'' (pH 7.4: mOsm 305; 2.5 mM K_2HPO_4; 2.0 mM $CaCl_2$; 1.2 mM $MgSO_4$; 5 mM glucose; 5.0 mM Na-acetate; 6 mM L-alanine; 1.0 mM Na_3-citrate; 115 mM NaCl; 4.0 mM Na-lactate; 0.5 mM *n*-butyric acid; 20 mM $NaHCO_3$; 14.1 mM raffinose) were prepared by dissolving increasing amounts of peptide directly in 0.1 ml of the above solution until no more went into solution. Samples were centrifuged for 3 min at 15,000 $\times$ *g*, and the supernatant was analyzed for protein concentration with the BCA protein assay (Pierce Chemical, Rockford, IL). Bovine serum albumin served as the protein standard and all peptide samples were corrected for dye binding differences that have been determined previously (4).

Cell culture

MDCK cells were a generous gift of Dr. Lawrence Sullivan (KUMC, Kansas City, KS) and were cultured as described previously (3). The HT-29 colon cancer parental cell line (ATCC No. HTB-38) was cultured in McCoy's 5a medium with 1.5 mM L-glutamine, 2.2 g/L sodium bicarbonate, 10% fetal bovine serum, in a humidified atmosphere of 95% air: 5% CO_2. Cells were plated at low density 12–18 h before electrophysiology experiments on sterile glass coverslips, which formed the bottom of the experimental chambers.

Chemicals

1-EBIO (Acros Organics, Division of Fischer Scientific, Pittsburgh PA) was prepared as a 1-M stock solution in dimethyl sulfoxide (DMSO)

(23,24). All other chemicals were purchased from Sigma-Aldrich Chemical (St. Louis, MO) and were of reagent grade unless otherwise noted.

Transepithelial ion transport measurements

Transepithelial ion transport was evaluated in a modified Ussing chamber (Model DCV9, Navicyte, San Diego, CA). For electrical measurements, MDCK cells were bathed in a modified Ringer solution ''B'' (120 mM NaCl, 25 mM $NaHCO_3$, 3.3 mM KH_2PO_4, 0.8 mM K_2HPO_4, 1.2 mM $MgCl_2$, and 1.2 mM $CaCl_2$ prepared fresh daily) (3) maintained at 37°C, and continuously bubbled with 5% CO_2/95% O_2 to provide aeration and mix the fluid in the chambers. The transepithelial membrane potential (V_{TE}) was clamped to zero and the *Isc* was measured continuously with a voltage clamp apparatus (Model 558C, University of Iowa, Department of Bioengineering, Iowa City, IA). Data acquisition was performed at 1 Hz with a Macintosh computer (Apple Computer, Cuppertino, CA) using Aqknowledge software (version 3.2.6, BIOPAC Systems, Santa Barbara, CA) with an MP100A-CE interface. *Isc* data are presented in tabular or bar chart forms at steady-state flux levels.

Ion transport data analysis

The data points represent the mean *Isc* stimulated by the peptide at concentrations between 10 and 500 μM and the error bars show the standard error of the mean. The differences between control and treatment data were analyzed using ANOVA and Student's *t*-test. The probability of making a type I error <0.05 was considered statistically significant. The lines are a best fit of a modified Hill equation to the data, $Isc = I_{MAX} \times (x^n/(K_{1/2}^n + x^n))$; where $K_{1/2}$ is the concentration of peptide that provides a half-maximal *Isc* and n represents the Hill coefficient.

Planar lipid bilayer experiments

Peptide ion channel activity was measured by planar lipid bilayer experiments. From supplied solutions (10 mg/mL in chloroform) of POPC (1-palmitoyl-2-oleoyl-*sn*-glycero-3-phosphocholine) and POPG (1-palmitoyl-2-oleoyl-*sn*-glycero-3-phospho-rac-(1-glycerol)) (Avanti Polar-Lipids, Alabaster, AL), a 70:30 molar ratio of POPC/POPG was prepared in chloroform. The lipid chloroform solution was evaporated under a stream of nitrogen and the lipids resuspended in 100 μL *n*-decane (Sigma) to a total lipid concentration of 10.0 mg/mL. Lipid bilayers composed of (70:30 mol ratio) were formed across a 150-μm aperture in the wall of a Delrin cup. The grounded electrode was applied to the *trans* side of the bilayer chamber with the voltage electrode applied to the *cis* side. Both the *cis* and *trans* chambers contained 0.1 M KCl connected by 1.0 M KCl agar bridges to the electrodes submerged in 2.0 M KCl. Lipids and peptide stock solutions were applied to the *cis* side of the bilayer apparatus. Bilayer current recordings were made with an EPC 9 patch clamp (HEKA; Lambert, Germany) and a Gould OS4100 digital storage oscilloscope (Cleveland, OH). The bilayer was conditioned and tested for stability and consistency before addition of peptide stock. Peptide was added by increments until sustained channel activity was observed.

Whole-cell patch-clamp analysis

The electrophysiology experiments were performed using standard high sodium, low potassium extracellular buffered saline solution and a high potassium buffered saline solution intracellularly. Intracellular calcium was maintained at 100 nM using EGTA and calcium saturated EGTA (25). The standard bath solution contained (in mM) 140 NaCl, 4.7 KCl, 1 $CaCl_2$, 1.1 $MgCl_2$, 10 HEPES (pH 7.4), and 10 glucose. In the ion-substituted buffers, K HEPES and NMDG HEPES, the NaCl was replaced by 140 KCl or 140 NMDG Cl, respectively. Pipette solution contained 20 NaCl, 40 KCl, 80 K glutamate, 10^{-4} $CaCl_2$, 1.1 $MgCl_2$, 10 HEPES (pH 7.4), and 10 glucose. Recording electrodes were pulled from borosilicate glass and fire polished to a resistance of 2–5 Ω when filled with the standard pipette solution. Whole cell currents were measured and recorded using a HEKA EPC 10 amplifier with Pulse software (version 8.76, HEKA Instruments, Southboro, MA). All recordings were obtained at 37°C by a water-jacketed perfusion system. Peptides were added to the experimental chamber by appropriate dilution with the flow stopped for 45–60 s, and then flow was resumed.

Whole-cell patched HT-29 cells were sequentially superfused with 140 mM NaCl HEPES, KCl HEPES, and NMDG Cl HEPES buffered saline. Pipette chloride was 60 mM, potassium 140 mM. Resting membrane potential (V_{mem}) varied between -35 and -55 mV ($n = 15$). Following bath exchange of NaCl for KCl, V_{mem} depolarized to 0 mV, subsequent cellular superfusion with NMDG Cl resulted in V_{mem} hyperpolarizing back to near initial conditions (25–45 mV, $n = 12$). Thus, under control conditions the membrane was selectively permeable to potassium>sodium, as predicted from previous studies. The channel-forming peptides were added directly to the bath solution once control whole-cell currents were established, and current-voltage relationships were monitored.

Chemical cross-linking reaction for M2GlyR related sequences

Bis-[sulfosuccinimidyl] suberate (BS^3) was purchased from Pierce. Precast 1.0 mm, 10 well, 10–20% tricine gels, tricine SDS buffer kit, Mark 12TM unstained standard, and SilverXpress silver staining kit were obtained from Invitrogen (Carlsbad, CA) and used as described previously (8). Cross-linking was performed using a 40-fold molar excess of BS^3 in Ringer Solution ''B'', as described previously (8,22).

Circular dichroism studies

Circular dichroism (CD) spectra were recorded in SDS micelles to monitor structural differences in secondary structure between the different NK_4-M2GlyR-p22 substituted sequences at 25°C in deionized, doubly distilled H_2O containing SDS micelles and 10 mM NaCl and 10 mM phosphate buffer pH 7.0 (Ultrapure grade from Sigma-Aldrich). Spectra were recorded on a Jasco J-720 spectropolarimeter with Neslab RTE-111M circulator using a cylindrical, water-jacketed, quartz cuvette with a 1.0-mm pathlength. Spectra shown are an average of eight scans recorded at a rate of 20 nm/min with a 1.0-nm step interval. Peptide concentrations of between 50 and 300 μM were used for the sequences in Tables 1–3. These concentrations cover the range over which biological activity is observed. Detergent monomer/peptide molar ratios of >200:1 were maintained. Peptide concentrations were determined with the Pierce BCA microprotein assay using a calibrated M2GlyR peptide solution as the standard (4). The concentration of the stock solution of NK_4-M2GlyR was determined using mol-percent ratios of the hydrolyzed PTC-amino acids by amino acid analysis. Data were analyzed using software provided by the manufacturer.

RESULTS AND DISCUSSION

Structure, activity, and solution association studies with M2GlyR derived peptides containing arginine at or near the C-terminus

In the native M2GlyR sequence an arginine residue is located near the C-terminus of the pore-forming TM segment. This residue was deleted when the peptide was truncated to 22 residues in length (8). Restoration of a positive charge near the C-terminus of the 22-residue peptide was tested with regard to increasing transport rates. A helical wheel projection of the M2GlyR-p22 helix reveals an even distribution of the polar

residues. Not knowing where to optimally substitute an arginine, a series of M2GlyR peptides was prepared with arginine replacing one amino acid in each of the five C-terminal sequence positions. These sequences are shown in Table 1 with their respective masses, solubility, and macroscopic kinetic constants that describe the relationships between apical peptide concentration and net ion transport rates across epithelial monolayers (Hill coefficient (n), Isc_{MAX}, and $K_{1/2}$). Sequence 1 is the unmodified NK_4-M2GlyR-p22 sequence, which displays nearly identical values for the Hill coefficient (n), Isc_{MAX}, and $K_{1/2}$ values, as does the full-length NK_4-M2GlyR-p27 (22). In sequences 2–6, the stepwise repositioning of the substituted arginine is shown. Substitution of the arginine at any of the shown positions raised aqueous solubility as expected, given the more hydrophilic nature of the arginine relative to that of the replaced amino acids. The greatest increase in solubility was observed when the hydrophobic residue methionine was replaced by arginine (sequence 6, Table 1).

The solution association properties of sequences 1–6 were examined using an amino-reactive bifunctional cross-linking reagent. These studies were undertaken to assess whether the introduction of an arginine at or near the C-terminus would also reduce solution associations. Peptide cross-linking studies using BS^3 revealed the presence of numerous water-soluble associations as assessed by silver stained polyacrylamide gel electrophoresis (similar to that shown in Fig. 5 in Broughman et al. (8)). A ladder of peptide associations was seen in the presence of the primary amine cross-linking agent. Monomer accounts for about half of the material observed in the individual gel lanes. In the absence of the cross-linker, SDS-containing loading buffer alone reduced the solution associations to the monomeric form. Clearly the introduction of an arginine anywhere within the five C-terminal residues has no effect on the intrinsic solution association properties of the nonsubstituted sequence (sequence 1). The soluble, yet highly associated, forms of the peptide are believed to be biologically inert, which impacts the concentration of bioactive material. The hydrophobic faces of the peptides are presumed to drive these associations (22). BS^3 has proven effective in trapping the associated forms of the lysine adducted channel-forming peptides (8,22). We see no evidence of recruitment of peptides to generate higher aggregates that are captured by a free half of the bifunctional cross-linker, as detected by mass spectrometry and SDS-PAGE analyses using either our sequences or melittin in concentration and time-dependence studies.

The secondary structures for sequences 1–6 were analyzed by CD in SDS micelles (20 mM) in the presence of 10 mM NaCl and 10 mM phosphate buffer pH 7.0. Under these conditions the SDS has a critical micellar concentration of 4.4 ± 0.3 mM as measured by isothermal calorimetry. The CD experiments for all sequences in this study were carried out in SDS micelles because they induce the greatest helicity for the different modified NK4-M2GlyR sequences when delivered from solution. In numerous structural studies, both NMR and CD, TFE and SDS micelles have been employed to mimic membrane environments (26–30). CD experiments were also conducted in extruded phospholipid micelles (POPC/POPS; 70:30), where peptide was delivered from solution. Under these conditions only beta-structure was observed. Some helical structures were obtained when the peptides were dried in the presence of the phospholipids before hydration and extrusion, but nothing approaching the values published in NMR structural studies on members of the cys-loop channel superfamily: glycine receptor (13,14) and nicotinic acetyl choline receptor (31). It appears that micelles prepared using two different phospholipids are not good models for the apical membrane of epithelium. Magzoub et al. (32) published a revealing report showing the variability in the secondary structure of the membrane active peptide ''penetratin'' (pAntp) in phospholipid liposomes (SUVs). The authors observed different peptide secondary structures (random coil, β, and helical) by varying the ratio of the different phospholipids (i.e., POPC/POPG) and peptide/lipid ratios.

Spectra were recorded for each sequence at 30–50 μM (Fig. 1) and 300 μM (not shown). Identical overlapping spectra were obtained for the individual sequences at all peptide concentrations and similar spectra were obtained for all substituted sequences. Peptide sequences 1–5 possessed some helical content, showing minima at 208 and 222 nm. The helical content for these sequences, as measured by CD, was consistent with that indicated by previous multidimensional NMR structural studies recorded with the native GlyR TM2 peptide dissolved in DPC micelles (13). Sequence 6 had minima that were slightly blue-shifted, 204 and 219 nm. This peptide showed no channel-forming activity (discussed

TABLE 1 Characterization of M2GlyR-p22 derived peptides with C-terminal arginines

Sequence	Replacement	Mr (Da)	Sol.(mM)	n	Isc_{MAX} (μA/cm^2)	$K_{1/2}$ (μM)
1. KKKKPA**R**VGLGITTVLTMTTQS	none	2358.9	11.1	1.9 ± 0.6	23.7 ± 5.6	210 ± 70
2. KKKKPA**R**VGLGITTVLTMTTQ**R**	S22R	2427.9	15.6	2.7 ± 0.9	24.1 ± 5.3	290 ± 60
3. KKKKPA**R**VGLGITTVLTMTT**R**S	Q21R	2387.0	19.7	2.2 ± 1.1	31.0 ± 18.0	390 ± 220
4. KKKKPA**R**VGLGITTVLTMT**R**QS	T20R	2414.0	18.7	1.3 ± 0.5	28.5 ± 14.8	310 ± 227
5. KKKKPA**R**VGLGITTVLTM**R**TQS	T19R	2414.0	18.3	0.7 ± 0.6	16.3 ± 3.5	120 ± 40
6. KKKKPA**R**VGLGITTVLT**R**TTQS	M18R	2383.9	23.3	0.6 ± 2.6	3.0 ± 4.0	840 ± 200

Sequences and physical and electrophysiological properties are shown. Bolded arginine residues define the putative TM segment. Isc_{MAX} is maximal anion flux and $K_{1/2}$ is the concentration required to obtain one-half of the maximal anion flux calculated based on the Hill equation using the data presented in Fig. 2.

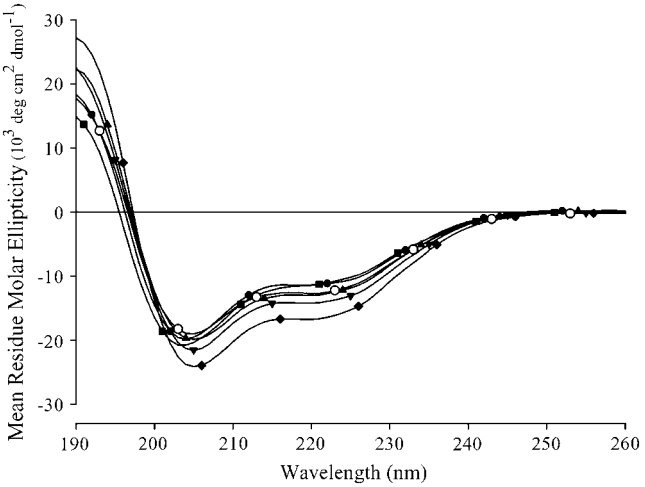

FIGURE 1 CD spectra of the arginine substituted NK_4-M2GlyR-p22. CD spectra of NK_4-M2GlyR wild type (sequence 1, Table 1) and arginine substituted sequences (sequences 2–6, Table 1) were recorded using 50 μM peptide in 10 mM sodium dodecylsulfate containing 10 mM NaCl and 10 mM phosphate buffer, pH 7.0, at room temperature (27–29°C). CD spectra for all peptides (sequences 1–6) are an average of eight data sets collected for each peptide. NK4-M2GlyR-derived peptides spectra are as follows: sequence 1 (○), sequence 2 (♦), sequence 3 (●), sequence 4 (▲), sequence 5 (▼), and sequence 6 (■).

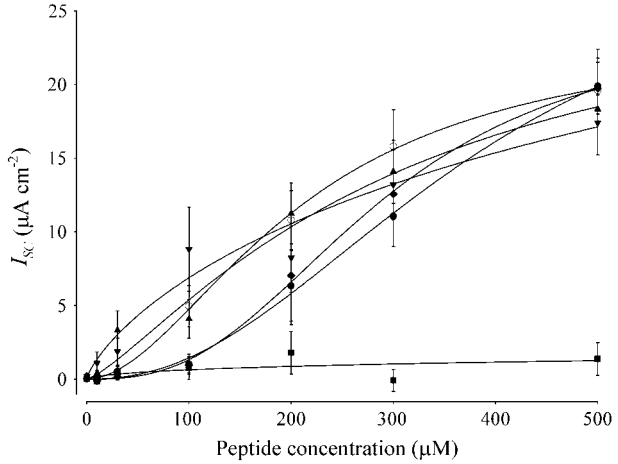

FIGURE 2 Concentration-dependence of *Isc* induced by NK_4-M2GlyR-p22 derived peptides with arginine replacement on MDCK epithelial monolayers. Symbols represent the mean and standard error of three to seven observations for each concentration tested. Solid lines represent the best fit of a modified Hill equation to each data set. The NK_4-M2GlyR derived peptides concentration dependent I_{SC} curves are as follows: sequence 1 (○), sequence 2 (♦), sequence 3 (●), sequence 4 (▲), sequence 5 (▼), and sequence 6 (■).

below). We speculate that the observed shift in the CD minima reflects an altered structure induced by a less favorable peptide/detergent micellar interaction.

The ability to induce anion secretion across epithelial monolayers was tested for sequences 1–6 (Table 1). Polarized epithelial cells (MDCK monolayers) were exposed to increasing concentrations of peptide sequences 1–6 in the presence of 1-EBIO (8,23,24) (Fig. 2). Table 1 also presents the summarized ion transport constants obtained for sequences 1–6 shown in Fig. 2. Introduction of an arginine residue to the NK_4-M2GlyR-p22 sequence in any one of the four C-terminal amino acid sites (sequences 2–5; Table 1) causes only subtle changes in maximal net ionic flux (*Isc*) or concentration dependence ($K_{1/2}$) relative to that seen for the wild-type sequence (sequence 1; Table 1). The calculated $K_{1/2}$ value is an indicator of the peptide affinity for supramolecular assembly. Addition of the Met-18Arg substituted peptide (sequence 6; Table 1) showed no increase in transport rates over pretreated values. Clearly replacing the hydrophobic methionine with a hydrophilic arginine was not well tolerated. Because the secondary structure (Fig. 1) for this sequence did not significantly differ from that of the active sequence 3, the defect in sequence six must lie in its inability to interact with the membrane or adversely effect supramolecular assembly.

Based on earlier studies (13–21,33) that describe the interfacial role of charged amino acids in TM segments, the endogenous arginine at position 7 and the newly introduced arginine in these substituted sequences are presumed to reside at the lipid/water interfaces. Evidence indicating that the role of the two arginines in defining the lipid/water interfaces is supported by the recently defined hydrophobic core spanning sequence of M2GlyR, based on NMR studies conducted in DPC micelles (13). This 18-residue segment is shown (underlined) within the wild-type TM2 sequence (PARVGLGITTVLTMTTQSSGSRA). In cases with the NK_4-M2GlyR-p22 substituted sequences, the absence of three of the predicted lipid spanning residues (boxed), present in the wild-type sequence, suggests that a different grouping of amino acids must span the membrane core. A core-spanning segment of 15 residues has been reported by others and is sufficient to produce a strong blue shift for an internal tryptophan (34). In this same study, an 11-residue peptide core was also able to span a detergent micelle that had lipid acyl chains made up of 16 carbon atoms.

Based on preliminary NMR and computer modeling studies of NK_4-M2GlyR-p22, it appears that the one or more of the N-terminal lysyl residues define the extracellular interfacial boundary. At the C-terminus, arginines substituted at positions 19–22 will position their guanido group at the lipid/water interface. Arginine at position 18 cannot. To maintain an 18-residue membrane spanning length, as the C-terminal arginine is positioned at residue 19, 20, 21, or 22, Arg-7 must be translocated partway down into the TM portion of the sequence and different lipid core embedded segments are defined by different N-terminal lysine anchors.

The inactivity of the Met-18 substitution is most likely due to lack of membrane insertion due to an energetically unfavorable positioning of the arginine within the acyl core of the bilayer or by requiring too many lysines to be accommodated within the lipid acyl core. Charged amino acid

residues are commonly found within transmembrane domains of transporters where they usually form a salt bridge with a residue of opposite charge (35–42). No such charge neutralization is possible in the homooligomer assembly. Snorkeling of the arginine and lysine side chains is restricted to sequence positions that are near the water lipid interface (43–45).

Based on the arginine substitution data for NK_4-M2GlyR-p22 series shown in Table 1, an arginine can be accommodated in any of the four C-terminal sites. Reintroduction of an arginine into those positions does not significantly alter the ion transport properties of the sequence in cultured epithelial cells. Although the arginine-substituted sequences have higher solubility, this property is not reflected in decreased solution associations of the peptides. If lipid core embedded sequence length is restricted to 18 residues, we postulate that as the position of existing or potential interfacial residues are relocated, altered assembly architectures with different helix anchors, helix pitch, helix angles, and different pore-lining residues must occur to maintain the transmembrane orientation. The apparent plasticity of the TM segment in altering its structure to maintain its perpendicular orientation can explain altered transport function in the NK_4-M2GlyR-p22 substituted homooligomeric assemblies.

Structure, activity, and solution association studies with M2GlyR derived peptides containing tryptophan with arginine residues at or near the C-terminus

Tryptophan was introduced into the NK_4-M2GlyR-p22 sequence to replace the C-terminal serine (sequence 7 in Table 2). This sequence, previously described in Cook et al. (22), was predominantly monomeric in solution and assembled into anion permselective channels at lower concentrations compared to the truncated wild-type peptide (sequence 1). However, the sequence attained only ~55% of the maximal anion current seen in the wild-type sequence.

A new series of double replacement peptides was prepared with tryptophan and arginine at selected locations within the last four positions in the C-terminus (Table 2). Arginine was substituted at Q21 (sequence 8), T20 (sequence 9), and T19 (sequence 10) while holding tryptophan at position 22. Sequence 11 was designed to test whether moving the arginine outside the membrane would produce a more stable channel based on thermodynamic considerations.

CD spectra for the tryptophan containing peptides at 50 μM and 300 μM were measured in 20 mM SDS in the presence of 10 mM NaCl and 10 mM phosphate buffer, pH 7.0 (not shown). No detectable changes in the CD spectra were recorded at either concentration. All peptides retained their overall helical secondary structure. None of the sequences possess >40% α-helical content in SDS, which is consistent with the previously discussed report showing the NMR structure of the M2GlyR segment recorded in SDS micelles (15). Structure was confined to only the transmembrane segment; residues outside of this hydrophobic environment were highly mobile, with no apparent stable structure (13,14). Within the lipid embedded segment, preliminary solution NMR results in both 40% TFE and SDS micelles suggest that the structured segment is bent and that only a portion of the segment is in a true α-helical conformation (13,14).

Fig. 3 shows the concentration dependence of the maximal ion transport rate for sequences 7–11 (Table 2). Table 2 presents the summarized ion transport kinetic constants from Fig. 3. The solid lines in the figure represent the best fit of a modified Hill equation to each data set. Sequence 1 displayed a concentration-dependent response similar to that observed with the 27-residue full-length CK_4-M2GlyR and NK_4-M2GlyR peptides (5,6). Sequence 1 provides benchmark values of Isc_{MAX} of 23.7 ± 5.6 $\mu A/cm^2$, $K_{1/2}$ of 210 ± 70 μM, and Hill coefficient of 1.9 ± 0.6.

Introduction of a tryptophan in the presence and absence of the added arginine (sequences 7–11, Table 2) had a dramatic effect on the concentration required for half-maximal ion transport activity. The left-shifted $K_{1/2}$ values ranged from 36 to 87 μM as compared with the 210 μM observed for the unmodified sequence 1. The four doubly substituted sequences (sequences 8–11, Table 2) exhibited similar left shifts in the $K_{1/2}$ for maximal anion transport as that measured for sequence 7, with a sole tryptophan substituted in position 22 (Table 2) and as recently reported (23). These sequences with left-shifted $K_{1/2}$ values form homooligomeric supramolecular assemblies at lower concentrations.

With regard to Isc_{MAX}, the doubly substituted sequences had increased maximal transport rates relative to either the

TABLE 2 Characterization of M2 derived peptides with tryptophan and arginine substitutions

Sequence	Replacement	Mr (Da)	Sol.(mM)	n	Isc_{MAX} ($\mu A\ cm^{-2}$)	$K_{1/2}$ (μM)
1. KKKKPARVGLGITTVLTMTTQS	none	2358.9	11.1	1.9 ± 0.6	23.7 ± 5.6	210 ± 70
7. KKKKPARVGLGITTVLTMTTQ**W**	S22W	2458.0	1.9	5.4 ± 2.9	13.0 ± 1.0	45 ± 6
8. KKKKPARVGLGITTVLTMTT**RW**	Q21R, S22W	2486.1	4.9	3.3 ± 1.6	26.5 ± 3.2	36 ± 5
9. KKKKPARVGLGITTVLTMT**RQW**	T20R, S22W	2513.1	5.2	2.3 ± 0.8	22.7 ± 2.7	87 ± 15
10. KKKKPARVGLGITTVLTM**R**TQ**W**	T19R, S22W	2513.1	5.1	3.5 ± 0.7	33.7 ± 1.3	71 ± 5
11. KKKKPARVGLGITTVLTMTT**WR**	Q21W, S22R	2486.0	22.0	3.8 ± 2.2	33.6 ± 2.2	55 ± 6

Sequences and physical and electrophysiological properties are shown. Isc_{MAX} is maximal anion flux and $K_{1/2}$ is the concentration required to obtain one-half of the maximal anion flux and are calculated based on the Hill equation using the data presented in Fig. 3.

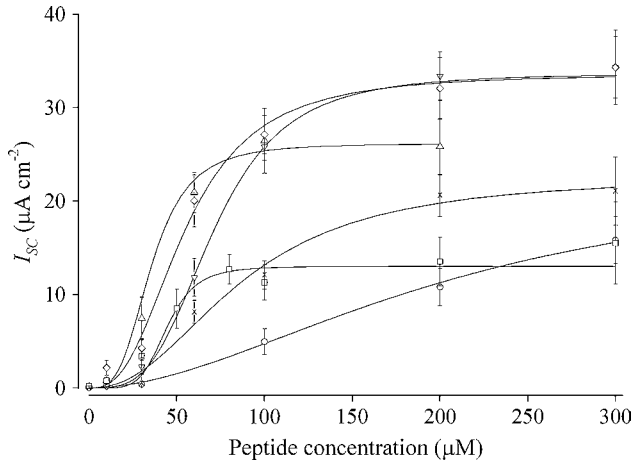

FIGURE 3 Concentration-dependence of *Isc* induced by NK_4-M2GlyR-p22 derived peptides with tryptophan and arginine amino acid substitutions on MDCK epithelial monolayers. Symbols represent the mean and standard error of six or greater observations for each concentration tested. Solid lines represent the best fit of a modified Hill equation to each data set. The NK_4-M2GlyR derived peptides dose dependent *Isc* curves are as follows: sequence 1 (○), sequence 7 (□), sequence 8 (△), sequence 9 (×), sequence 10 (▽), and sequence 11 (◇).

wild-type (sequence 1) or C-terminal tryptophan substituted (sequence 7) peptides. In the doubly substituted sequences the position of the arginine relative to the tryptophan also had an effect on Isc_{MAX}. In sequences 8 and 9 introduction of arginine at positions 20 or 21 was associated with a greater Isc_{MAX} (22.7 ± 2.7 and 26.5 ± 3.2 μA/cm^2, respectively) over that seen with the tryptophan alone substituted sequence. These Isc_{MAX} values are similar to that seen for the wild-type M2GlyR-p22 (sequence 1). Introduction of the arginine at position 19 (sequence 10) and inverting the arginine-tryptophan pair of sequence 8 to tryptophan-arginine (sequence 11) resulted in even larger Isc_{MAX} values of 33.7 ± 1.3 and 33.6 ± 2.2 μA/cm^2, respectively. Most importantly, sequences 8–11 showed greatly enhanced efficacy with *Isc* values equaling Isc_{MAX} for sequence 1 with concentrations at or below 50 μM. The sum effect of changes in the kinetic parameters (Isc_{MAX} and $K_{1/2}$) is a substantial reduction in the peptide concentration required to attain anion secretion rates that will likely be relevant in future basic research and applied applications. Sequences 7, 8, 10, and 11 have greater Hill coefficients (5.4 ± 2.9, 3.3 ± 1.6, 3.5 ± 0.7, and 3.8 ± 2.2, respectively) than that calculated (1.9 ± 0.6) for sequence 1. Sequence 9 has a Hill coefficient (2.3 ± 0.8) similar to that seen with sequence 1. The increase in the Hill coefficients to values approaching five suggests that association/dissociation mechanisms in the bilayer are sensitive to structural changes in the peptide and consistent with the prediction that the channel pore is a homo-oligomeric supramolecular assembly.

Two processes are postulated to account for the decrease in the concentration required for half-maximal activity ($K_{1/2}$). Firstly, the presence of a tryptophan residue eliminates the formation of higher molecular weight associations in aqueous environments. This effectively increases the concentration of soluble monomer, proposed to be the most membrane active species (22). Secondly, the propensity of tryptophan to reside at the aqueous/lipid interface (18–21) could set the registry of the transmembrane segment that spans the bilayer. In the absence of an arginine or aromatic residue at or near the C-terminus the peptide could rise up and down within the fluid bilayer thereby affecting the depth of peptide insertion into the membrane and tilt angle of the peptide. By providing a membrane anchor at position 22, a reduction in the degrees of freedom for the transmembrane registry of the peptide would occur thereby facilitating assembly at lower concentrations.

As assessed in the Ussing chamber experiments, reintroduction of an arginine near the C-terminus contributes a third factor that influences the minimum concentrations required for assembly. Introduction of an arginine, at any of the tested positions, slightly decreases the Hill coefficient, suggesting that there is an energetic cost in forcing the arginines (transiently) across the acyl core of the phospholipids. Placing the arginines at either position 19 or just outside the membrane appears to be optimal with regard to Isc_{MAX}. Placing the arginine at position 21 appears to be optimal with regard to $K_{1/2}$. Placing the arginine at position 20 seems to be the least optimal position since the Hill coefficient, $K_{1/2}$ and Isc_{MAX} show the lowest values within this peptide series. Preliminary computer modeling studies indicate that the arginine in any of the internal C-terminal positions could snorkel back toward the membrane to form a second membrane anchor. There is no evidence that any of the substituted arginines, in sequences 8–11, are positioned with the side chain pointed into the water-filled lumen of the assembled pore.

Single channel recordings obtained in phospholipid bilayers for sequences 7–11 are shown in Fig. 4. Although all sequences form de novo channels, the single channel properties such as conductance, open probability, and open times are different for each of the sequences. All of the amino acid substituted sequences described in this report are able to self-assemble in phospholipid bilayers and provide new conductance pathways, which can account for the peptide-induced transepithelial ion transport in intact epithelium. These results are consistent with those obtained for the longer CK_4-M2GlyR-p27 (5) and NK_4-M2GlyR-p27 (6).

Structure, activity, and solution association studies with M2GlyR derived peptides containing phenylalanine or tyrosine with arginine residues at or near the C-terminus

To better understand the role of indole-containing peptides in lowering $K_{1/2}$ values, new sequences were prepared that replaced the tryptophan with either phenylalanine or tyrosine

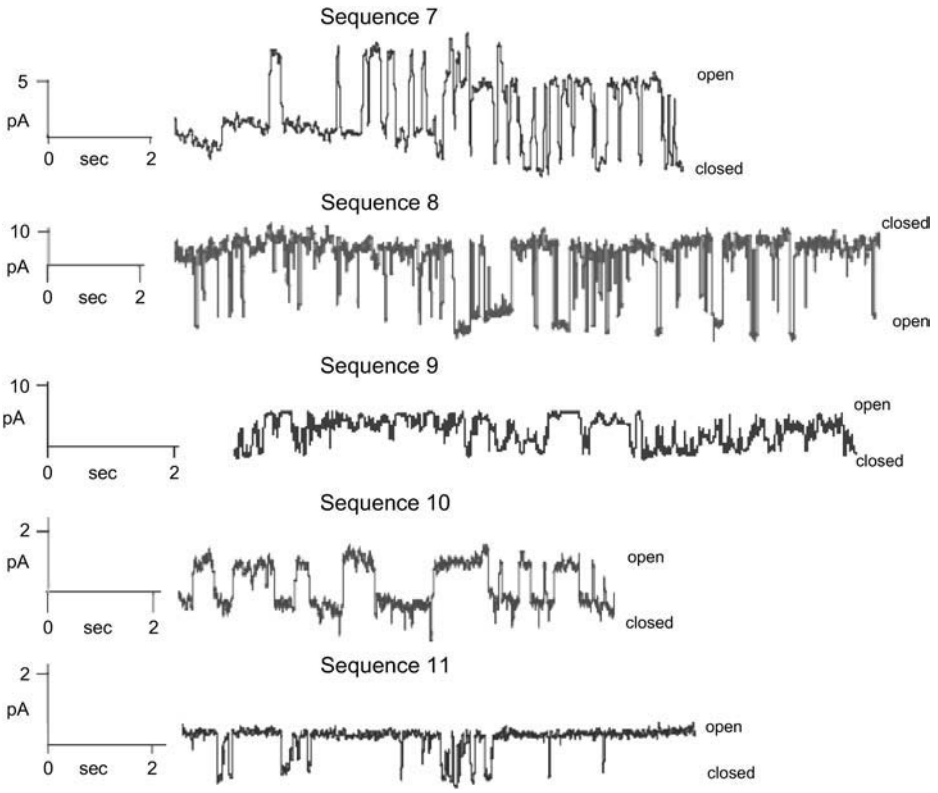

FIGURE 4 Single-channel recordings of tryptophan and arginine substituted NK_4-M2GlyR peptides in synthetic bilayers. Channel recordings were made in symmetrical 100 mM KCl at 80 mV with a peptide concentration of 1.0 μM at room temperature for all sequences with the exception of sequence 8, which was recorded at −80 mV. The bilayer composition was 70:30 POPC/POPG for all samples.

(sequences 12–16, Table 3). These substitutions were prepared to assess whether any aromatic amino acid (Phe, Tyr, or Trp) at the C-terminus: 1), increases monomer concentrations, 2), alters secondary structure, or 3), sets the registry of the peptide within the bilayer.

The phenylalanine or tyrosine substituted sequences, which also contain a second arginine substitution (sequences 12–16, Table 3), displayed increased solubility compared to their tryptophan containing counterparts with the exception of sequence 14, the phenylalanine-containing counterpart of sequence 11. These two sequences had the same solubility (21 vs. 22 mM). All of the aromatic containing sequences had lesser amounts of higher molecular weight associations in aqueous environments (Fig. 5) compared to the aromatic free sequence (sequence 1, Wallace et al. (24)). Predominantly monomer, with some dimer, is present in the cross-linked aromatic sequences.

Secondary structures in SDS micelles were measured, as before, for sequences 12–16 (Table 3) at both 50 and 300 μM. The CD scans (not shown) for these sequences were similar to those seen for the arginine-substituted series (Fig. 1) and the tryptophan containing sequences. All of the Table 3 sequences had recorded minima at 208 and 222 nm.

Considering the lack of solution aggregation and similar CD profiles, we conclude that these sequences form a similar hydrophobic fold (in solution) that prevents higher associations, similar to that observed by Cook et al. (22) for sequence 7. Besides improving the concentration of monomer in aqueous solutions, inclusion of any C-terminal aromatic residue provides a lipid/water interfacial anchor. In addition to tryptophan, phenylalanine residues are commonly found (and tyrosine to a lesser extent) at the hydrophobic/hydrophilic interface for transmembrane segments of membrane proteins (3–6).

TABLE 3 Characterization of peptides with phenylalanine/tyrosine and arginine substitutions

Sequence	Replacement	Mr (Da)	Sol.(mM)	n	Isc_{MAX} (μA cm^{-2})	$K_{1/2}$ (μM)
12. KKKKPARVGLGITTVLTMTT**RF**	Q21R, S22F	2447.1	6.1	3.8 ± 2.5	21.3 ± 2.5	56 ± 8
13. KKKKPARVGLGITTVLTM**R**TQ**F**	T19R, S22F	2474.1	12.2	2.3 ± 0.3	38.0 ± 2.3	120 ± 14
14. KKKKPARVGLGITTVLTMTT**FR**	Q21F, S22R	2447.1	21.0	3.1 ± 0.6	31.8 ± 3.6	120 ± 10
15. KKKKPARVGLGITTVLTMTT**RY**	Q21R, S22Y	2463.1	26.9	2.4 ± 0.6	29.4 ± 3.1	98 ± 14
16. KKKKPARVGLGITTVLTM**R**TQ**Y**	T19R, S22Y	2490.1	24.5	2.3 ± 0.8	18.3 ± 2.9	110 ± 23

Sequences and physical and electrophysiological properties are shown. Isc_{MAX} is maximal anion flux and $K_{1/2}$ is the concentration required to obtain one-half of the maximal anion flux and are calculated based on the Hill equation using the data presented in Fig. 6.

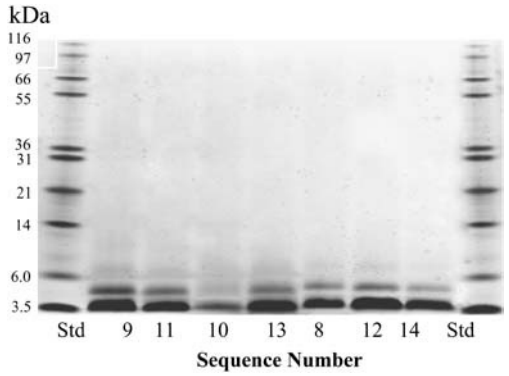

FIGURE 5 Cross-linking study of arginine and aromatic substituted peptides in solution. Tricine 10–20% gradient polyacrylamide gel of cross-linking patterns NK_4-M2GlyR-p22 derived peptides with aromatic and arginine amino acid substitutions (150 μM) treated with a 40-fold excess of cross-linking reagent in Ringers buffer ''B''. Peptides treated with BS3 are labeled according to the sequence numbers given in Tables 2 and 3. The protein bands are visualized using silver stain.

The *Isc* versus concentration data for sequences 12–16 are shown in Fig. 6, with the n, Isc_{MAX} and $K_{1/2}$ values summarized in Table 3. The data for sequences 1 and 11 are included in the figure for reference. Comparing the phenylalanine variants (sequences 12–14) to the paired tryptophan containing sequences 8, 10, and 11, the phenylalanine-containing peptides displayed similar Isc_{MAX} but right-shifted $K_{1/2}$ values. The tyrosine variants (sequences 14 and 15) of sequences 8 and 10 gave mixed results relative to their tryptophan counterparts. Sequence 15 showed a higher

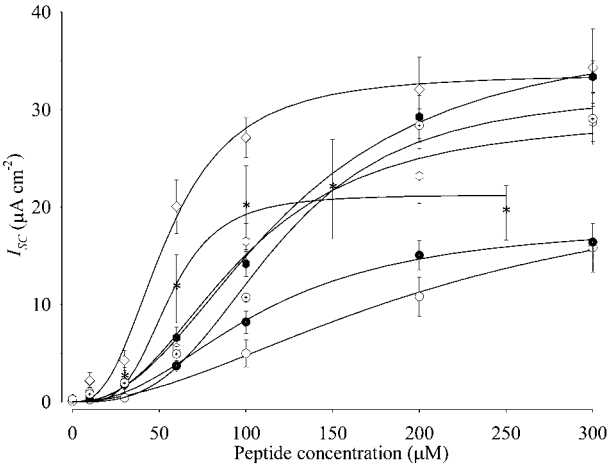

FIGURE 6 Concentration-dependence of *Isc* induced by NK_4-M2GlyR p22 derived peptides with either phenylalanine or tyrosine and arginine amino acid substitutions on MDCK epithelial monolayers. Symbols represent the mean and standard error of four or greater observations for each concentration tested. Solid lines represent the best fit of a modified Hill equation to each data set. The NK_4-M2GlyR derived peptides dose-dependent *ISC* curves are as follows: sequence 1 (○), sequence 11 (◇), sequence 12 (*), sequence 13 (⬬), sequence 14 (⊕), sequence 15 (⬭) and sequence 16 (◘).

Isc_{MAX} but right-shifted $K_{1/2}$ value whereas sequence 16 was inferior in both respects. With the exception of sequence 12, the $K_{1/2}$ values for the tyrosine and phenylalanine containing peptides are right-shifted relative to the tryptophan containing peptides but left-shifted relative to the unmodified M2GlyR-p22 (sequence 1).

Comparing all of the summarized data in Tables 2 and 3 and the profiles shown in Figs. 3 and 6, the sequences displaying the highest ion transport activity and the second and third most-left-shifted $K_{1/2}$ values are both tryptophan-containing peptide sequences (sequences 10 and 11). Based on the concentrations required for $K_{1/2}$, a rank ordering of the assembly promoting effects of the C-terminal aromatic substitutions are as follows Trp $>$ Phe $\gg$ Tyr.

Increased anion secretion necessarily reflects changes in underlying biophysical parameters of the epithelial system. Equation 1 shows that the net current, I, reflects the product of the unitary current (i) (the product of electrical potential, V, and conductance, g, by Ohms law; Eq. 2), the number of actively gating channels, N, and the probability of a channel being in a conducting (i.e., open) state, P_o.

$$I = iNP_o, \tag{1}$$

where,

$$i = gV. \tag{2}$$

Channels dissipate electrical gradients regardless of their conductance or number so long as a portion of the channels are in a conducting state (i.e., $P_o > 0$). Thus, the elevated net currents induced by many of the modified sequences presented here, cannot reflect a channel-induced increase in the electrochemical driving force, V. Furthermore, the selected experimental conditions are included to standardize the net driving force for anion secretion by including 1-EBIO to maintain an elevated electrochemical driving force. Thus, differences in maximal current between channel-forming peptides, as observed in Fig. 3, could reflect differences in unitary conductance, maximal number of active channels, differences in P_o, or some combination of these possibilities. Because saturation is observed with all peptides tested, one must conclude that some maximal number of channels is conducting anions at any point in time. The possibility that anion loading limits net secretion is ruled out for any situation in which $<\sim 30\ \mu A\ cm^{-2}$ is observed. Results from studies employing sequence 10 (Fig. 3), and previously reported observations (7,8) demonstrate that MDCK monolayers are routinely capable of secreting anions at a rate $>30\ \mu A\ cm^{-2}$. Thus, results suggest that either the conductance, maximal number of channels, or open probability is reduced for the other sequences shown in Figs. 3 and 6. A combination of these effects could also account for these results. Differences in the Hill coefficient might suggest that alternative numbers of monomers associate in the membrane to form active channels. Thus, at a saturating peptide concentration in the membrane, differing numbers of channels

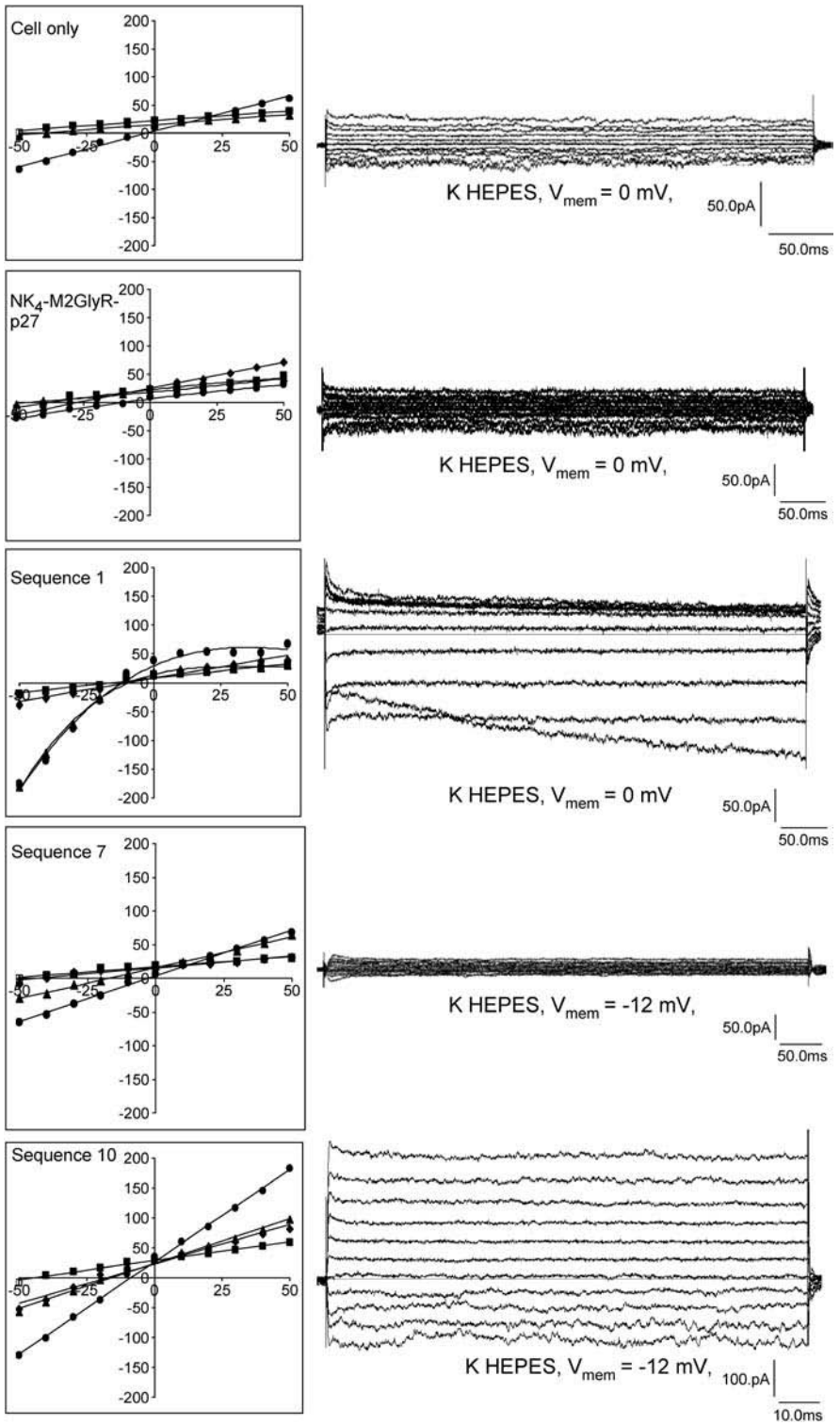

FIGURE 7 Current-voltage relationships: patched HT-29 cells (control conditions) were sequentially superfused with 140 mM NaCl (■), KCl (●), and NMDG Cl (▲) HEPES buffered saline solutions. The pipette holding potential was increased stepwise from either −50 to +50 mV in 10 mV steps. Treatment conditions (NK_4-M2GlyR-p27, sequences 1, 7, and 10) Channel-forming peptides were added directly to the bath chamber after a whole-cell patch was obtained (■). Upon formation of stable channels (♦), NaCl HEPES buffer bathing the cell was exchanged for KCl buffer (●) followed by NMDG Cl buffer (▲). Representative current overlays for the K HEPES bath are shown to the right. The pipette contained K^+ and reduced Cl^- (see Experimental Section). Whole-cell currents were measured in pA.

may form and channels with different stoichiometries might exhibit unique conductances and gating kinetics. We are using analytic ultracentrifugation studies in micelles to verify the existence of assemblies with different oligomerization states. Alternatively, one might postulate that associated forms of some sequences are both conductive and particularly stable resulting in an elevated P_o. The unitary conductance may also differ depending on the sequence although we view it as unlikely that anion-selective trimers, tetramers, and pentamers would form. One might hypothesize that introduction of the new amino acids at the C-terminus alter both the sequence of the embedded segment within the

hydrophobic core as well as the pore-lining residues thereby modulating the throughput of the channel. We are currently mapping the pore-lining residues in NK_4-M2GlyR-p22 S22W, T19R (sequence 10) using a cysteine scanning approach to address this alternative hypothesis. These studies are beyond the scope of this work.

Lastly, an ion selectivity study was performed on the full-length NK_4-M2GlyR-p27 (22) as well as sequences 1, 7, and 10 (Fig. 7 and Table 2) in a whole-cell membrane patch-voltage clamp experiment using a human colonic carcinoma cell line (HT-29). These results give an indication of the type of changes that are induced by the amino acid replacements discussed in this study. NK_4-M2GlyR-p27, sequence 1, and sequence 10 increased whole-cell conductance two- to fourfold over baseline and induced a left-shift in the whole-cell reversal potential in the presence of Na^+ or $NMDG^+$ as the predominant bath cation, suggesting a cation permselectivity sequence of $K^+ \gg Na^+ > NMDG^+$. With symmetrical K^+ gradients, reversal potentials were approximately zero for the untreated cells and for sequence 7. NK_4-M2GlyR-p27, sequence 1, and sequence 10, however, exhibited reversal potentials that were negative, consistent with substantial Cl^- permeability. These data suggest a Cl^- permselectivity sequence of NK_4-M2GlyR-p27 > sequence 10 = sequence 1 > sequence 7, although additional work is required to fully characterize the biophysical fingerprint of these channel sequences. The inward rectification of sequence 1 in K^+ and $NMDG^+$ baths and time-dependent activation at negative potentials suggests that additional channels are being recruited into the membrane (increased N in Eq. 1) or that an alternative conductance (with increased i) becomes favored in these conditions. These observations will prove useful in the design of channels with rectifying characteristics. Nonetheless, the current experiments identify sequence 10 as a lead compound for channel replacement therapy studies. This peptide shows three desirable characteristics: is monomeric in solution; inserts in membrane and assembles at low aqueous concentrations; and exhibits Cl^- selectivity. The inclusion of the arginine at residue 19 results in a significant increase in transport rates with some loss of selectivity. Introduction of a presumed second anchor appears to alter the overall structure of the assembled channel. Preliminary NMR structural studies indicate that adding the arginine at position 19 changes the secondary structure of the peptide.

SUMMARY

The peptides described in this report represent novel designs with unique activities. The authors are unaware of anyone else systematically dissecting a native channel-forming sequence to study the structural elements that drive assembly, ion selectivity, and conductance. All of the sequences described herein are water-soluble monomers that, when exposed to membranes, insert and then undergo supramolecular assembly to form testable bioactive structures. These derived sequences show a wide range of new properties and structures that have application as new materials as well as potential as therapeutic agents.

The results presented in this study reveal important properties about transmembrane peptides derived from the GlyR M2 sequence. When applied to symmetrical symmetrical bilayers or the apical surface of epithelial monolayers, the derived sequences insert and then assemble into homooligomeric helical bundles to give ion transport activities that can be measured across the treated membrane. The activities observed vary from peptide to peptide, thereby providing a system by which channel-forming tendencies can be studied and optimized in a reductionist manner. The self-assembling GlyR M2 derived sequences have been shortened and modified through an iterative process such that a water-soluble peptide is easily deliverable to membrane surfaces from aqueous solution while maintaining channel activity.

Charged amino acids such as arginine, and to a greater extent aromatic amino acids such as phenylalanine and tryptophan, help to define the registry of the acyl core embedded segment. Placing the tryptophan C-terminally to the arginine can lead to the incorporation of that arginine within the bilayer with the subsequent snorkeling back of its guanido group back toward the lipid/water interfacial zone to form a second anchor and perhaps distort the helix TM orientation. Peptides of uniform sequence length but with differing acyl embedded segments would therefore produce channels with altered channel geometries and pore-lining residues.

Placement of an aromatic residue at the C-terminus eliminates all of the high molecular weight associations of the peptide thereby increasing the concentration of the biologically active form. The 22-residue peptide sequences KKKKPARVGLGITTVLTMRTQW and KKKKPARVGLGITTVLTMTTWR reveal themselves as the most potent channel-forming sequences, showing high levels of ion transport activity at a peptide concentration of 60 μM and attaining a maximum anion current of 34 $\mu A\ cm^{-2}$ in epithelial monolayers. The sequence, KKKKPARVGLGITTVLTMTTQW, reaches maximal activity at ~80 μM with an improved efficacy as measured by the 6.2-fold decrease in $K_{1/2}$ concentration over that of the full-length NK_4-M2GlyR-p27 (22) with retention of anion selectivity. The peptides displaying the higher currents appear to be nonselective. Experiments are under way to determine the structure of these sequences in SDS micelles as well as to introduce amino acid substitutions in pore-lining residues to improve anion selectivity for the sequences with higher transport rates.

The authors are grateful to Ryan Carlin for technical assistance and Professor A. P. Morris for use of his patch rig by J.R.B.

The work is supported by the National Institute of General Medical Sciences, grants GM43617 and GM 074096 (J.M.T.). This work is contribution 02-466-J from the Kansas Agricultural Experiment Station (J.M.T. and B.D.S.).

REFERENCES

1. Cragg, P. J. 2002. Artificial transmembrane channels for sodium and potassium. *Sci. Prog.* 85:219–241.
2. Reddy, L. G., T. Iwamoto, J. M. Tomich, and M. Montal. 1993. Synthetic peptides and four-helical bundle proteins as model systems for the pore-forming structure of channel proteins. III. Transmembrane segment M2 of the brain glycine receptor channel is a plausible candidate for the pore-lining structure. *J. Biol. Chem.* 268:14608–14615.
3. Wallace, D. P., J. M. Tomich, T. Iwamoto, K. Henderson, J. J. Grantham, and L. P. Sullivan. 1997. A synthetic peptide derived from glycine-gated Cl^- channel induces transepithelial Cl^- and fluid secretion. *Am. J. Physiol.* 272:C1672–C1679.
4. Tomich, J. M., D. P. Wallace, K. Henderson, K. E. Mitchell, G. Radke, R. Brandt, C. A. Ambler, A. J. Scott, J. J. Grantham, L. P. Sullivan, and T. Iwamoto. 1998. Aqueous solubilization of transmembrane peptide sequences with retention of membrane insertion and function. *Biophys. J.* 74:256–267.
5. Mitchell, K. E., T. Iwamoto, J. M. Tomich, and L. C. Freeman. 2000. A synthetic peptide based on a glycine-gated chloride channel induces a novel chloride conductance in isolated epithelial cells. *Biochim. Biophys. Acta.* 1466:47–60.
6. Broughman, J. R., K. E. Mitchell, R. L. Sedlacek, T. Iwamoto, J. M. Tomich, and B. D. Schultz. 2001. NH_2-terminal modification of a channel-forming peptide increases capacity for epithelial anion secretion. *Am. J. Physiol. Cell Physiol.* 280:C451–C458.
7. Broughman, J. R., L. P. Shank, T. Iwamoto, O. Prakash, B. D. Schultz, J. M. Tomich, and K. E. Mitchell. 2002. Structural implications of placing cationic residues at either the NH_2- or COOH− terminus in a pore-forming synthetic peptide. *J. Membr. Biol.* 190:93–103.
8. Broughman, J. R., L. P. Shank, W. Takeguchi, T. Iwamoto, K. E. Mitchell, B. D. Schultz, and J. M. Tomich. 2002. Distinct structural elements that direct solution aggregation and membrane assembly in the channel forming peptide M2GlyR. *Biochemistry.* 41:7350–7358.
9. Wimley, W. C., and S. H. White. 1996. Experimentally determined hydrophobicity scale for proteins at membrane interfaces. *Nat. Struct. Biol.* 3:842–848.
10. Wimley, W. C., and S. H. White. 1999. Membrane protein folding and stability: physical principles. *Ann. Rev. Biophys. Biomol. Struct.* 28: 319–365.
11. Wimley, W. C., and S. H. White. 2000. Designing transmembrane α-helices that insert spontaneously. *Biochemistry.* 39:4432–4442.
12. Jayasinghe, S., K. Hristova, and S. H. White. 2001. Energetics, stability, and prediction of transmembrane helices. *J. Mol. Biol.* 312: 927–934.
13. Tang, P., P. K. Mandal, and Y. Xu. 2002. NMR structures of the second transmembrane domain of the human glycine receptor alpha(1) subunit: model of pore architecture and channel gating. *Biophys. J.* 83:252–262.
14. Yushmanov, V. E., P. K. Mandal, Z. Liu, P. Tang, and Y. Xu. 2003. NMR structure and backbone dynamics of the extended second transmembrane domain of the human neuronal glycine receptor alpha1 subunit. *Biochemistry.* 42:3989–3995.
15. Vogt, B., P. Ducarme, S. Schinzel, R. Brasseur, and B. Bechinger. 2000. The topology of lysine-containing amphipathic peptides in bilayers by circular dichroism, solid-state NMR, and molecular modeling. *Biophys. J.* 79:2644–2656.
16. Harzer, U., and B. Bechinger. 2000. Alignment of lysine-anchored membrane peptides under conditions of hydrophobic mismatch: a CD, 15N and 31P solid-state NMR spectroscopy investigation. *Biochemistry.* 39:13106–13114.
17. Mitaku, S., T. Hirokawa, and T. Tsuji. 2002. Amphiphilicity index of polar amino acids as an aid in the characterization of amino acid preference at membrane-water interfaces. *Bioinformatics.* 18:608–616.
18. Demmers, J. A., E. van Duijn, J. Haverkamp, D. V. Greathouse, R. E. Koeppe 2nd, A. J. Heck, and J. A. Killian. 2001. Interfacial positioning and stability of transmembrane peptides in lipid bilayers studied by combining hydrogen/deuterium exchange and mass spectrometry. *J. Biol. Chem.* 276:34501–34508.
19. Mall, S., R. Broadbridge, R. P. Sharma, A. G. Lee, and J. M. East. 2000. Effects of aromatic residues at the ends of transmembrane alpha-helices on helix interactions with lipid bilayers. *Biochemistry.* 39:2071–2078.
20. de Planque, M. R., B. B. Bonev, J. A. Demmers, D. V. Greathouse, R. E. Koeppe 2nd, F. Separovic, A. Watts, and J. A. Killian. 2003. Interfacial anchor properties of tryptophan residues in transmembrane peptides can dominate over hydrophobic matching effects in peptide-lipid interactions. *Biochemistry.* 42:5341–5348.
21. Braun, P., and G. von Heijne. 1999. The aromatic residues Trp and Phe have different effects on the positioning of a transmembrane helix in the microsomal membrane. *Biochemistry.* 38:9778–9782.
22. Cook, G. A., O. Prakash, K. Zhang, L. P. Shank, A. Robbins, Y.-X. Gong, T. Iwamoto, B. D. Schultz, and J. M. Tomich. 2004. Activity and structural comparisons of solution associating and monomeric channel-forming peptides derived from the glycine receptor M2 segment. *Biophys. J.* 86:1424–1435.
23. Devor, D. C., A. K. Singh, R. J. Bridges, and R. A. Frizzell. 1996. Modulation of Cl^- secretion by benzimidazolones. I. Direct activation of a Ca^{2+}-dependent K+ channel. *Am. J. Physiol.* 271:L775–L784.
24. Wallace, D. P., J. M. Tomich, J. W. Eppler, T. Iwamoto, J. J. Grantham, and L. P. Sullivan. 2000. A synthetic channel-forming peptide induces Cl^- secretion: modulation by Ca+-dependent K+ channels. *Biochim. Biophys. Acta.* 1464:69–82.
25. Morris, A. P., K. L. Kirk, and R. A. Frizzell. 1990. Simultaneous analysis of cell Ca^{2+} and $Ca^{2(+)}$-stimulated chloride conductance in colonic epithelial cells (HT-29). *Cell Regul.* 1:951–963.
26. Thevenin, D., T. Lazarova, M. F. Roberts, and C. R. Robinson. 2005. Oligomerization of the fifth transmembrane domain from the adenosine A2A receptor. *Protein Sci.* 14:2177–2186.
27. Castiglione-Morelli, M. A., A. Ostuni, F. Croce, F. Palmieri, and F. Bisaccia. 2005. Solution structure of the fifth and sixth transmembrane segments of the mitochondrial oxoglutarate carrier. *Mol. Membr. Biol.* 22:191–201.
28. Castiglione-Morelli, M. A., A. Ostuni, A. Pepe, G. Lauria, F. Palmieri, and F. Bisaccia. 2004. Solution structure of the first and second transmembrane segments of the mitochondrial oxoglutarate carrier. *Mol. Membr. Biol.* 21:297–305.
29. Crowell, K. J., C. M. Franzin, A. Koltay, S. Lee, A. M. Lucchese, B. C. Snyder, and F. M. Marassi. 2003. Expression and characterization of the FXYD ion transport regulators for NMR structural studies in lipid micelles and lipid bilayers. *Biochim. Biophys. Acta.* 1645:15–21.
30. Raghuraman, H., and A. Chattopadhyay. 2004. Effect of micellar charge on the conformation and dynamics of melittin. *Eur. Biophys. J.* 33:611–622.
31. Montal, M., and S. J. Opella. 2002. The structure of the M2 channel-lining segment from the nicotinic acetylcholine receptor. *Biochim. Biophys. Acta.* 1565:287–293.
32. Magzoub, M., L. E. Eriksson, and A. Graslund. 2002. Conformational states of the cell-penetrating peptide penetratin when interacting with phospholipid vesicles: effects of surface charge and peptide concentration. *Biochim. Biophys. Acta.* 1563:53–63.
33. Esposito, G., B. Dhanapal, P. Dumy, V. Varma, M. Mutter, and G. Bodenhausen. 1997. Lysine as helix C-capping residue in a synthetic peptide. *Biopolymers.* 41:27–35.
34. Ren, J., S. Lew, J. Wang, and E. London. 1999. Control of the transmembrane orientation and interhelical interactions within membranes by hydrophobic helix length. *Biochemistry.* 38:5905–5912.
35. Jarolim, P., H. L. Rubin, V. Brabec, L. Chrobak, A. S. Zolotarev, S. L. Alper, C. Brugnara, H. Wichterle, and J. Palek. 1995. Mutations of conserved arginines in the membrane domain of erythroid band 3 lead to a decrease in membrane-associated band 3 and to the phenotype of hereditary spherocytosis. *Blood.* 85:634–640.

36. Muller, V., G. Basset, D. R. Nelson, and M. Klingenberg. 1996. Probing the role of positive residues in the ADP/ATP carrier from yeast. The effect of six arginine mutations of oxidative phosphorylation and AAC expression. *Biochemistry.* 35:16132–16143.

37. Steiner-Mordoch, S., A. Shirvan, and S. Schuldiner. 1996. Modification of the pH profile and tetrabenazine sensitivity of rat VMAT1 by replacement of aspartate 404 with glutamate. *J. Biol. Chem.* 271:13048–13054.

38. Merickel, A., H. R. Kaback, and R. H. Edwards. 1997. Charged residues in transmembrane domains II and XI of a vesicular monoamine transporter form a charge pair that promotes high affinity substrate recognition. *J. Biol. Chem.* 272:5403–5408.

39. Fei, Y. J., W. Liu, P. D. Prasad, R. Kekuda, T. G. Oblak, V. Ganapathy, and F. H. Leibach. 1997. Identification of the histidyl residue obligatory for the catalytic activity of the human H+/peptide cotransporters PEPT1 and PEPT2. *Biochemistry.* 36:452–460.

40. Kavanaugh, M. P., A. Bendahan, N. Zerangue, Y. Zhang, and B. I. Kanner. 1997. Mutation of an amino acid residue influencing potassium coupling in the glutamate transporter GLT-1 induces obligate exchange. *J. Biol. Chem.* 272:1703–1708.

41. Sharina, I. G., R. Zhao, Y. Wang, S. Babani, and I. D. Goldman. 2001. Mutational analysis of the functional role of conserved arginine and lysine residues in transmembrane domains of the murine reduced folate carrier. *Mol. Pharmacol.* 59:1022–1028.

42. Lew, S., J. Ren, and E. London. 2000. The effects of polar and/or ionizable residues in the core and flanking regions of hydrophobic helices on transmembrane conformation and oligomerization. *Biochemistry.* 39:9632–9640.

43. Monne, M., I. Nilsson, M. Johansson, N. Elmhed, and G. von Heijne. 1998. Positively and negatively charged residues have different effects on the position in the membrane of a model transmembrane helix. *J. Mol. Biol.* 284:1177–1183.

44. Strandberg, E., S. Morein, D. T. Rijkers, R. M. Liskamp, P. C. van der Wel, and J. A. Killian. 2002. Lipid dependence of membrane anchoring properties and snorkeling behavior of aromatic and charged residues in transmembrane peptides. *Biochemistry.* 41:7190–7198.

45. Strandberg, E., and J. A. Killian. 2003. Snorkeling of lysine side chains in transmembrane helices: how easy can it get? *FEBS Lett.* 544:69–73.